J Radioanal Nucl Chem (2013) 295:929–935
DOI 10.1007/s10967-012-1908-6

Synthesis and characterization of magnetic nano-material for removal of Eu^{3+} ions from aqueous solutions

S. I. Moussa · R. R. Sheha · E. A. Saad · N. A. Tadros

Received: 9 May 2012 / Published online: 3 July 2012

Abstract Ferrite coated apatite magnetic nano-material was synthesized by a co-precipitation method and applied in removal of Eu(III) ions from aqueous solutions. The sample was firstly characterized using Fourier transform infrared spectroscopy, thermogravimetric analyses, deferential thermal analysis, X-ray powder diffraction, surface area by nitrogen adsorption and scanning electron microscopy. The results of physicochemical properties indicated that the synthesized magnetic nano-adsorbent had a crystalline structure and possessed a surface area amounted to 85.11 m^2 g^{-1}. Further, it was found to have high thermal resistance up to 600 °C and mean particle size of about 63 nm. The kinetic of Eu(III) sorption indicated that equilibrium state was attained within 12 h with using 5 mg as an appropriate nano-adsorbent weight. The sorption process was pH and ionic strength dependent. The maximum adsorbed amount of Eu(III) was attained at pH 2.5 with value reached to 157.14 mg g^{-1}. Desorption of Eu(III) from loaded samples was studied using various eluents and maximum recovery was obtained using $FeCl_3$ solution.

Keywords HAP · Fe_3O_4 · Magnetic nanoparticles · Eu(III) ions · Adsorption

S. I. Moussa · R. R. Sheha (✉) · N. A. Tadros
Nuclear Chemistry Department, Hot Labs. Center, AEA, PO 13759 Cairo, Egypt
e-mail: reda.sheha@eaea.org.eg

E. A. Saad
Department of Chemistry, Faculty of Science, Ain Shams University, Cairo, Egypt

Introduction

The environmental behavior of lanthanide and actinide ions has attracted a wide attention because they are the main constituents of long-lived radioactive wastes. In addition, sorption and transport behavior of long-life radionuclides on hydrological environment are an important issue in performance and safety assessment of nuclear waste repositories [1, 2]. Among lanthanides, europium is a trivalent element could be considered as a chemical homologue to trivalent lanthanides. Also, it has a sorption behavior similar to that of the trivalent actinides at natural water–solid interface [3]. Removal of lanthanides from waste solutions can be achieved by several processes such as chemical reduction [4], solvent extraction [5], ion exchange [6] or adsorption [7, 8]. Among them, sorption technique seems to be a promising approach could offer a number of benefits such as reducing solvent usage, disposal costs and extraction time.

Nowadays, the technologies based on magnetic separation are an efficient, fast and economical method for environmental purification. Hence, many research efforts are directed to combine magnetic separation with adsorptive removal in purification processes [9–11]. It was selectively applied in industrial, biological, and environmental processes [12–14]. Biologically, magnetic nanoparticles have promising applications in cell separation and drug delivery. In addition, they were effectively used as a contrast agent for magnetic resonance imaging and a heat mediator for hyperthermia [15–17].

Hydroxyapatites were widely applied in environmental purification purposes and exhibited a remarkable ability to absorb heavy metal ions, such as Cd^{2+} [18, 19], Co^{2+} [20], Pb^{2+} [21, 22], Zn^{2+} [21, 23] and Cu^{2+} [21, 24]. Also, magnetic iron oxides could be used as a support material in

preparation of many composite adsorbents because it can be easily manipulated by an external magnetic field [25]. Recently, several studies was carried out on surface modification of Fe_3O_4 nanoparticles to effectively applied in removal of different heavy metals [26–28]. In this concern, Feng et al. [29] synthesized magnetic hydroxyapatite nanoparticles for removal of Cd^{2+} and Zn^{2+} from aqueous solution. Further, Dong et al. [30] combined HAP with Fe_3O_4 to produce composite absorbent for removal of heavy metals from aqueous solutions. The removal of Eu(III) from aqueous solution using Fe_3O_4 coated HAP as adsorbents have never been reported in the literature. Therefore, this study aims to prepare ferrite nanoparticles coated with calcium hydroxyapatites and assess its potential application in removal of $^{152+154}$Eu isotopes from aqueous solution.

Experimental

Synthesis of sorbent

All chemicals used throughout this study were of analytical grade, and used as received without further purification. Iron ferrite (Fe_3O_4) was prepared using a co-precipitation method. A solution of 1 M $FeCl_3$ was stirred and purged with N_2 at 25 ± 1 °C. To this solution, an equal volume of 0.5 M $FeSO_4{\cdot}7H_2O$ solution was added slowly under continuous stirring and nitrogen flow to have Fe(II):Fe(III) molar ratio 2:1. The mixture was stirred and purged with N_2 for 30 min at 25 ± 1 °C and then NH_4OH solution (25 %) was added until pH attended 11. Then, a black precipitate was formed and let to settle down. The precipitate was separated by filtration, washed several times with distilled water and finally heated at 80 °C for 1 h till pH attained a constant around ~7.

A solution of 0.5 M $Ca(NO_3)_2$ was stirred and purged with N_2 at 25 ± 1 °C. An equal volume of 0.387 M $(NH_4)_2HPO_4$ was added slowly to this solution under continuous stirring and N_2 flow. The molar ratio of Ca/P was kept at 1.67 and the mixture was stirred and purged with N_2 at 25 ± 1 °C for 30 min. To ferrite suspension, the previously prepared mixture was added slowly under continuous stirring and nitrogen flow for 30 min. Thereafter, NH_4OH solution (25 %) was added until pH value reached to about 11. The resulting precipitate was separated by filtration, washed several times with bidistilled water until pH became 7 and finally dried at room temperature for 48 h.

Radioactive tracer

Radioactive isotopes of $^{152+154}$Eu were prepared by neutron irradiation using the Egyptian Second Research Reactor at Inshas, Egypt. A weight of 1 mg (Eu_2O_3) was wrapped in a thin aluminum foil and irradiated using 10^{14} ns^{-1} cm^{-1} neutron flux. After cooling, the sample was dissolved in 1 M HCl, evaporated to dryness and redissolved in double distilled water. The activity of the prepared isotopes was γ-counted using NaI scintillation counter connected to nuclear single channel (Spectech ST 360, USA).

Characterization

The synthesized particles were characterized using the following techniques. Fourier transform infrared (FT-IR) spectra were recorded with Nicolet is10 spectrometer from Meslo, USA. Thermal analysis was carried out using Shimadzu TGA/DTA-50 system. Thermogravimetric analysis/deferential thermal analysis (TGA/DTA) measurements were done up to a temperature of 600 °C, with a heating rate of 10 °C min^{-1} in a nitrogen atmosphere, and using α-Al_2O_3 as a reference. X-ray analysis was performed with X'Pert diffractometer system of PW1710 model, from Philips, Almelo, Netherlands. The specific surface area and porosity of the samples were determined by the standard adsorption of N_2 at 77 K, using a sorptometer of the type NOVA 1000e model Quantachrome, USA. The morphology of prepared particles was observed using Jeol scanning electron microscope JSM-6510A model, Japan.

Sorption experiment

The variation in the amount adsorbed with time was studied by shaking 5 mg sample with 5 ml of 200 ppm Eu(III) in a thermostatic shaker at 25 ± 1 °C. After equilibrium, the adsorbent was separated by centrifuge and the supernatant was subjected to radiometrical assay. To clarify the effect of sample weight, different sample weights ranged from 0.001 to 0.025 g were used with 200 ppm Eu(III) solution. The mixtures were shaken at room temperature for 48 h, separated and analyzed to determine the amount adsorbed from europium ions. In addition, the effect of pH was studied within the pH range of 0.5–4. The initial metal concentration was 200 mg l^{-1}, while the initial pH values were adjusted by adding NaOH or HCl solutions. After 48 h of contact, the suspensions were separated and analyzed for final pH value and the activity of europium.

The amount adsorbed (q_e) in mg g^{-1} was measured by repeated equilibration with 200 ppm europium chloride solutions spiked with $^{152+154}$Eu at an initial pH of 2.5, in a thermostat shaker adjusted at 25 ± 1 °C. The *V*/*m* ratio was 1,000 ml g^{-1} and each equilibration was continued for 48 h. The equilibration was repeated until no further uptake of Eu(III) took place. Certain volumes of

supernatant were withdrawn, counted for γ-activity and replaced with an equal volume of the original solution. The amount adsorbed was calculated using the equation:

$$q_e = [C_o - C_e] \times V/m \quad (1)$$

where C_o and C_e are the initial and final Eu(III) concentration in solution (mg l^{-1}), V is the volume of solution (ml) and m is the weight of the sample (g).

Desorption study was performed by equilibrating 10 ml of 200 mg l^{-1} Eu(III) solution with 0.1 g sample in a set of glass bottles. Subsequently, the suspension was centrifuged and supernatants were separated and assayed. The solid residues were thoroughly treated with 10 ml of six different leaching solutions in six sealed glass bottles and were shaken for 24 h. The eluent were 0.05 M HCl, H_2O, 0.1 M NaOH, 0.1 M $CaCl_2$, 0.1 M $FeCl_2$ and 0.1 M $FeCl_3$ solutions. Finally, the suspensions were centrifuged and the activity of metal ion, desorbed in solution, was analyzed.

Results and discussion

Characterization

FT-IR

Infrared spectra of the prepared adsorbent are shown in Fig. 1. The plot exhibited a broad absorption band around 3,400 cm^{-1} may be due to presence of structural hydroxyl groups. The bands revealed at 1,634 and 634 cm^{-1} are characteristic to Fe_3O_4 [31]. The peaks exhibited at 1,000–1,100 and 560–610 cm^{-1} could be attributed to the presence of PO_4^{3-} group [32]. The bands observed at 1,092 and 1,034 cm^{-1} are due to the stretching vibration of phosphate (PO_4^{3-}, P–O) groups while the bands detected at 601 and 563 cm^{-1} may be ascribed to the bending vibration of phosphate (PO_4^{3-}, O–P–O). These bands are characteristic to hydroxyapatite structure. The broad band detected between 3,460 and 3,400 cm^{-1} are indicative to the existence of the bending mode of absorbed water in the sample [33].

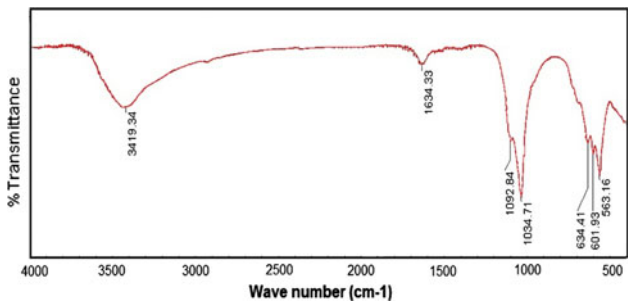

Fig. 1 FT-IR spectrum of the synthesized magnetic nano-adsorbent

Thermal analysis

The thermograms of the synthesized particles are shown in Fig. 2. The TG exhibited a decrease in sample weight with rising temperature up to ~120 °C. This weight loss was accompanied with an endothermic peak revealed at 78 °C. This endothermic peak implied the dehydration of surface water molecules. With rising temperature up to 260 °C, the sample approximately showed a thermal stability with no DTA peaks. A further decrease in sample weight was observed with increasing temperature up to 330 °C. This loss was accompanied with an endothermic peak at 274 °C. This could be attributed to the dehydration of water molecules impeded in internal structure. At high temperature up to 600 °C, the sample showed a continuous stability with no weight loss.

X-ray analysis

Figure 3 shows the X-ray powder diffraction pattern of: (a) sample as prepared and (b) sample calcinated at 250 °C. The diffractograms clarified that the sample is predominantly hydroxyapatites and are consistent with JCDP data of ASTM card No. 9-432 for HAP and ASTM card No. 19-629 of Fe_3O_4. The plots authenticate that sample calcination at 250 °C improved the peaks sharpness and hence the structure crystallinity. This improvement in properties could be ascribed to the dehydration of water molecules from the internal structure.

Surface area measurement

The values of specific surface area (S_{BET}) and porosity are given in Table 1. The BET surface area was 85.11 m^2 g^{-1}. This value is higher than that reported by other investigators for different HAP samples [34–36].

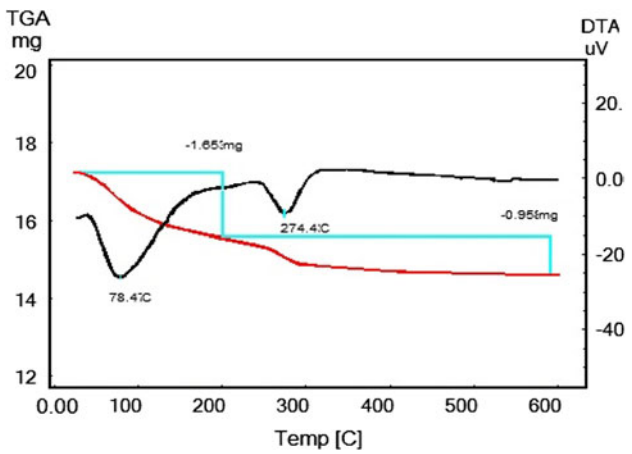

Fig. 2 TG–DTA of the synthesized magnetic nano-adsorbent

Scanning electron microscope (SEM)

The morphology of the prepared magnetic particles at different magnification powers is shown in Fig. 4. The pictures showed that the synthesized adsorbent had irregular spherical shape with average diameter of about 63 nm. Also, they had a rough surface and porous structure.

Sorption study

Contact time

The change in the amount adsorbed of Eu(III) with time was studied using batch technique and data are given in Fig. 5. Data illustrated that the removal of Eu(III) by magnetic nano-adsorbent took place in two steps: a relatively fast step, followed by a slow one extended until the equilibrium was reached. The time necessary to reach the equilibrium was about 12 h. Though there, a slight increase of adsorption quantity after 24 h was detected. Therefore, 48 h was considered as a time of contact in the rest of experiment. The maximum adsorbed amount of europium ions was determined experimentally through successive sorption and the values are listed in Table 2. The revealed data clarified that the prepared magnetic nano-adsorbent exhibited a higher sorption capacity compared with other materials.

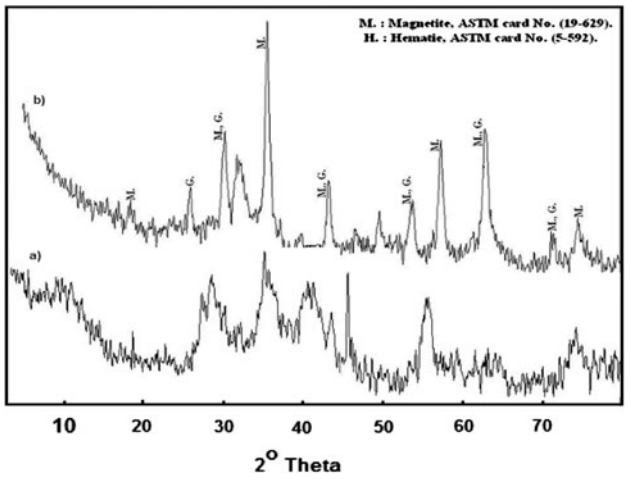

Fig. 3 X-ray diffraction patterns of the synthesized magnetic nano-adsorbent: *a* sample as prepared, *b* sample calcinated at 250 °C

Table 1 The textural properties of the synthesized magnetic nano-adsorbent

Samples	Surface area parameter			Reference
	S_{BET} ($m^2\ g^{-1}$)	V_P ($cm^3\ g^{-1}$)	D_P (nm)	
Mag nano sorbent	85.11	0.099	23.26	This work
HAP	51.8	–	–	[34]
HAP	67	–	–	[20]
HAP	48	–	141.3	[35]
HAP	43.75	–	–	[36]

Effect of sample weight

The relationship between sample weight and the amount of Eu(III) adsorbed using the prepared magnetic nano-sample is shown in Fig. 6. It was observed that, the amount adsorbed increased with increasing the weight of nano-sample up to 0.01 g while at higher amounts, q_e values remained constant. Closer inspection to data clarified that, the amount adsorbed attained the value of 155.14 mg g^{-1} with 5 mg of sample weight while it attained 198.42 mg g^{-1} at 10 mg sample. Therefore, the increase in q_e values from 155.14 to 198.42 mg g^{-1} was not consisted with the increase in sample weight from 5 to 10 mg. So, it was supposed to consider 5 mg as a sample weight in the rest of experiments.

Effect of pH value

Sorption of europium by prepared magnetic nano-adsorbent was studied at different pH value ranged from 0.5 to 4 and the results are show in Fig. 7. It is clear that, the amount adsorbed of Eu(III) increased with increasing pH value up to 2.5. At high pH value, q_e value decreased with the increase in pH value up to 4.5 after which q_e attained a constant value. This behavior could be attributed to changing the speciation products and the involved sorption mechanism at the solid–liquid interface with changing the pH value. Further, the values of final pH increased with increasing the initial pH values up to 3.7. After which the final pH value remain constant. This behavior could be assigned the buffering properties of HAP [18]. The buffering characteristics of HAP were a result of acid–base interactions due to the exchange with Eu(III).

Effect of ionic strength

The Effect of ionic strength, adjusted with NaCl salt, on Eu(III) sorption onto prepared magnetic nano-adsorbent is presented in Fig. 8. Data clarified that q_e of Eu(III) decreased with increasing ionic strength molarity. This was because the movement of Eu(III), from bulk solution towards adsorbent surface, was retarded with presence of increased concentration of Na(I) ions that formed a positive layer on the surface of applied nano-adsorbent. Also, Na(I) could competes with Eu(III) for the available active

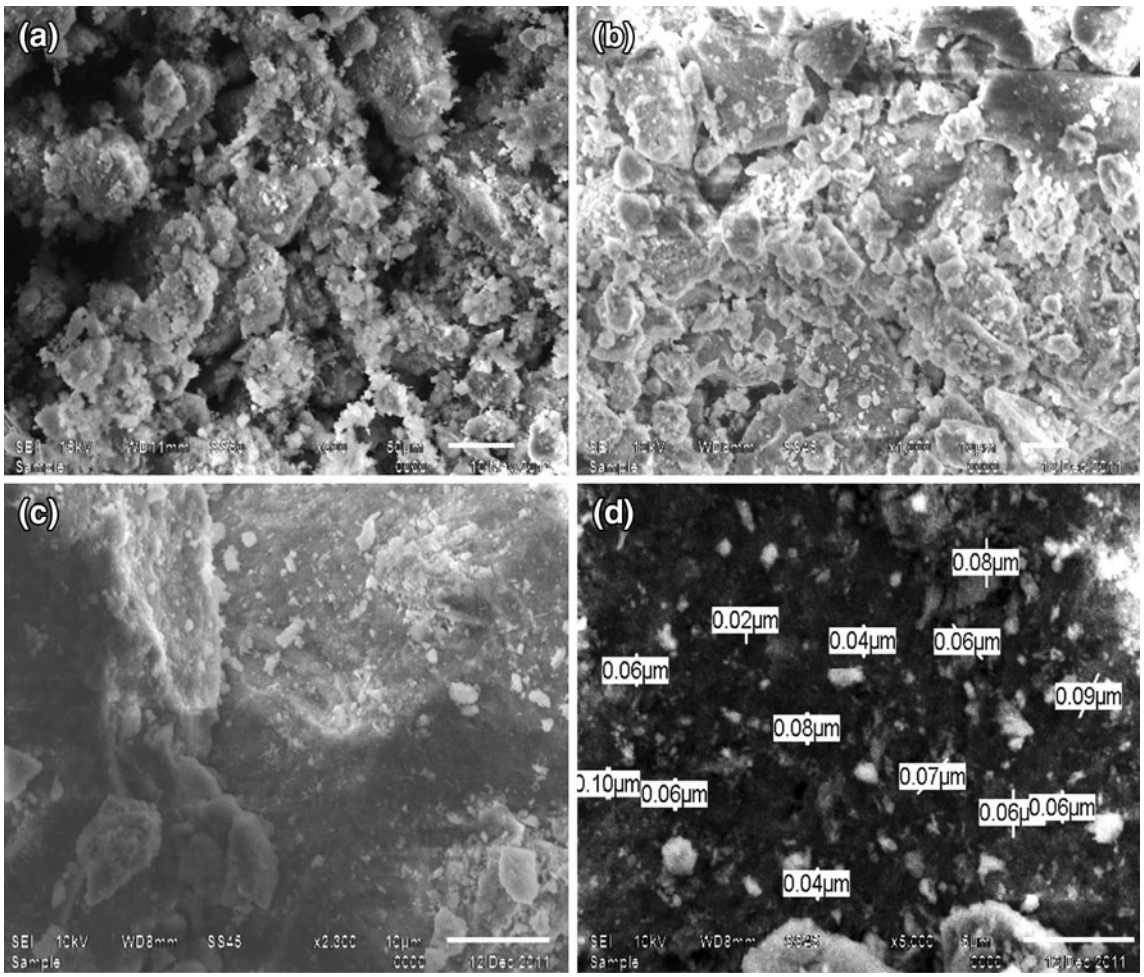

Fig. 4 SEM micrograph of the synthesized magnetic nano-adsorbent at zoom: **a** 300, **b** 1000, **c** 2300 and **d** 5000

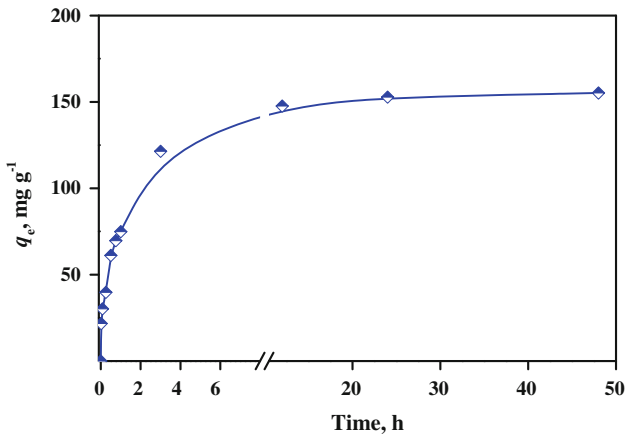

Fig. 5 Variation of Eu(III) adsorbed onto synthesized magnetic nano-adsorbent with time

sites on adsorbent surface. It worse to note that the high ionic charge of Eu(III) ions compared with that of Na(I) ions, depressed the competition action of Na(I) ions therefore, the overall q_e values were slightly decreased with presence of increased concentration of NaCl as a background electrolyte.

Table 2 The sorption capacity of the synthesized magnetic nano-adsorbent

Sample	q_e (mg g^{-1})	References
Mag nano sorbent	157.14	This work
GMZ bentonite	40.5	[37]
Activated carbon	18.41	[38]
CA	9.35	[39]
CA/AAm	19.08	[39]
CA/PEG	27.40	[39]

Desorption study

The results of desorption study are shown in Fig. 9. The data illustrated that Eu(III) was hardly eluted from the

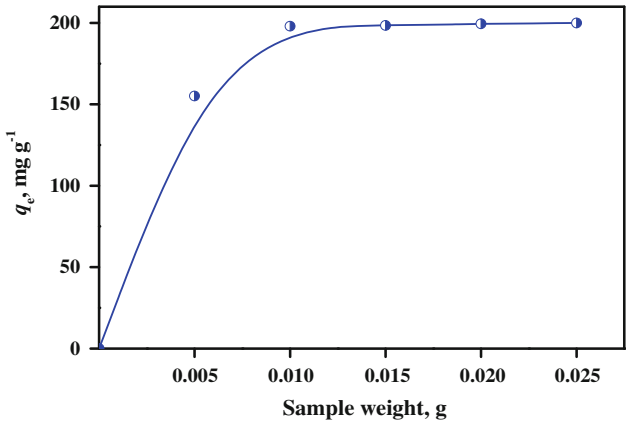

Fig. 6 Variation of Eu(III) adsorbed onto synthesized magnetic nano-adsorbent with sample weight

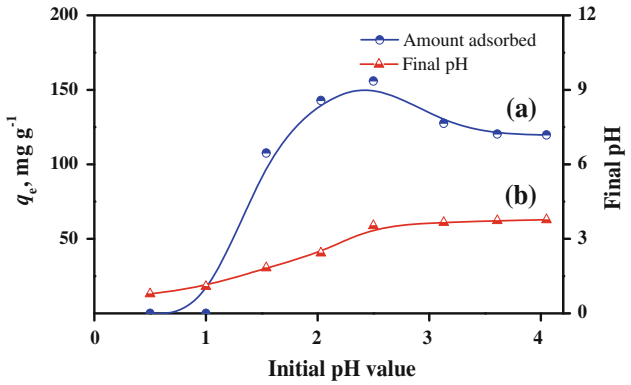

Fig. 7 Variation of Eu(III) adsorbed onto synthesized magnetic nano-adsorbent with initial pH value

magnetic nano-adsorbent using distilled water, 0.1 M $CaCl_2$ and NaOH. On other hand, it was easily desorbed using 0.05 M HCl, 0.1 M $FeCl_2$ and $FeCl_3$ solutions. The desorption percentages of Eu(III) eluted from the applied magnetic nano-adsorbent were 71.75, 86.13, 98.99, 2, 3 and 1.3 % by using 0.05 M HCl, 0.1 M $FeCl_2$, $FeCl_3$, 0.1 M NaOH, 0.1 M $CaCl_2$ and H_2O, respectively. A similar result was reported for Zn(II) desorption from loaded CaHAP [23].

The high desorption yield reveled with $FeCl_3$ could be ascribed to the chemical properties of Fe(III) ions compared with Eu(III) ions. Both ions have a comparable ionic radius ($r_{Eu(III)} = 0.95$ Å, $r_{Fe(III)} = 0.64$ Å) while Fe(III) ions have a high surface electronegativity amounted to 1.8 Pauling compared with that of Eu(III) that attain the value 1.2 Pauling. This difference in electronegativity enabled Fe(III) ions to effectively replace Eu(III) from the active site present on the surface of magnetic nano-adsorbent. In addition, the low ionic radius of Fe(III) ions facilitates such proposed replacement. Based on these data, the adsorbed Eu(III) ions can be effectively recovered from

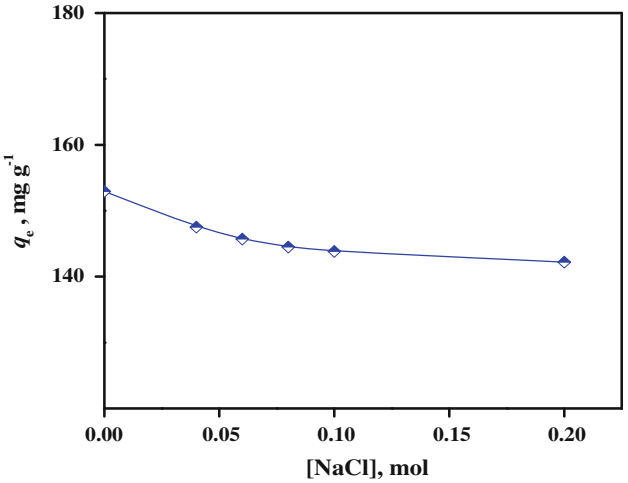

Fig. 8 Variation of Eu(III) adsorbed onto synthesized magnetic nano-adsorbent with presence of NaCl as back ground electrolyte

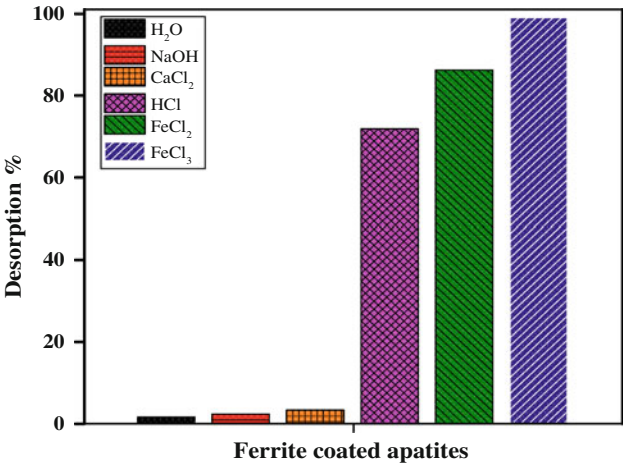

Fig. 9 Desorption behavior of Eu(III) from loaded samples using different eluents

the synthesized adsorbent using $FeCl_3$. Further, the results highlight the promising application of this nano-material in separation and recovery of lanthanide elements from their aqueous solutions.

Conclusions

In this study, a magnetic nano-adsorbent composed from iron ferrite core and hydroxyapatite shell was successfully synthesized. The prepared nano-material had a high thermal stability and possessed a crystalline structure. The sorption of Eu(III) was highly attained from acid solution and slightly affected by the value of ionic strength. The elution of Eu(III) loaded in presented sample was highly recovered using the eluent, HCl, $FeCl_2$, $FeCl_3$. The results highlight the promising application of this material in

separation and recovery of lanthanide elements from their aqueous solutions.

References

1. Fan QH, Zhang ML, Zhang YY, Ding KF, Yang ZQ, Wu WS (2010) Radiochim Acta 98:19–25
2. Shao DD, Fan QH, Li JX, Niu ZW, Wu WS, Chen YX, Wang XK (2009) Microporous Mesoporous Mater 123:1–9
3. Tan X, Fang M, Li J, Lu Y, Wang X (2009) J Hazard Mater 168:458–465
4. Morais CA, Ciminelli VST (2001) Hydrometallurgy 60:247–253
5. Bhattacharyya A, Mohapatra PK, Gadly T, Raut DR, Ghosh SK, Man-chanda VK (2011) J Hazard Mater 95:238–244
6. Jelinek L, Wei YZ, Arai T, Kumagai M (2008) J Alloy Compd 451:341–343
7. Sharma P, Singh G, Tomar R (2009) J Colloid Interface Sci 332:298–308
8. Guerra DL, Viana RR, Airoldi C (2010) Desalination 260:161–171
9. Ai ZH, Cheng Y, Zhang LZ, Qiu JR (2008) Environ Sci Technol 42:6955–6960
10. Pal S, Alocilja EC (2009) Biosens Bioelectron 24:1437–1444
11. Rocher V, Siaugue JM, Cabuil V, Bee A (2008) Water Res 42:1290–1298
12. Gong JL, Wang B, Zeng GM, Yang CP, Niu CG, Niu QY, Zhou WJ, Liang Y (2009) J Hazard Mater 164:1517–1522
13. Zhang GS, Qu JH, Liu HJ, Liu RP, Wu RC (2007) Water Res 41:1921–1928
14. Zhang GS, Liu HJ, Liu RP, Qu JH (2009) J Colloid Interface Sci 335:168–174
15. Mornet S, Vasseur S, Grasset F, Duguet E (2005) J Biosci Bioeng 100:1–11
16. Pankhurst QA, Connolly J, Jones SK, Dobson J (2003) J Phys D Appl Phys 36:167–181
17. Kalambur VS, Han B, Hammer BE, Shield TW, Bischof JC (2005) Nanotechnology 16:1221–1233
18. Zhu RH, Yu RB, Yao JX, Mao D, Xing CJ, Wang D (2008) Catal Today 139:94–99
19. Corami A, Mignardi S, Ferrini V (2008) J Colloid Interface Sci 317:402–408
20. Smiciklas I, Dimovic S, Plecas I, Mitric M (2006) Water Res 40:2267–2274
21. Smiciklas I, Onjia A, Raicevic S, Janackovic D, Mitric M (2008) J Hazard Mater 152:876–884
22. Kaludjerovic-Radoicica T, Raicevic S (2010) Chem Eng J 160:503–510
23. Sheha RR (2007) J Colloid Interface Sci 310:18–26
24. Sljivic M, Smiciklas I, Plecas I, Mitric M (2009) Chem Eng J 148:80–88
25. Chang YC, Chang SW, Chen DH (2006) React Funct Polym 66:335–341
26. Banerjee SS, Chen DH (2007) J Hazard Mater 147:792–799
27. Yantasee W, Warner CL, Sangvanich T, Addleman RS, Carter TG, Wiacek RJ, Fryxell GE, Timchalk C, Warner MG (2007) Environ Sci Technol 41:5114–5119
28. Huang SH, Chen DH (2009) J Hazard Mater 163:174–179
29. Feng Y, Gong J, Zeng G, Niu Q, Zhang H, Niu C, Deng J, Yan M (2010) Chem Eng J 162:487–494
30. Dong L, Zhu Z, Qiu Y, Zhao J (2010) Chem Eng J 165:827–834
31. Yu SY, Zhang HJ, Yu JB, Wang C, Sun LN, Shi WD (2007) Langmuir 23:7836–7840
32. Mobasherpour I, Heshajin MS, Kazemzadeh A, Zakeri M (2007) J Alloy Compd 430:330–333
33. Wu HC, Wang TW, Sun JS, Wang WH, Lin F-H (2007) Nano-technology 18:165601 (p 9)
34. Gomez del Rio JA, Morando PJ, Cicerone DS (2004) J Environ Manag 71:169–177
35. Mostafa NY (2005) Mater Chem Phys 94:333–341
36. Lin K, Pan J, Chen Y, Cheng R, Xu X (2009) J Hazard Mater 161:231–240
37. Chen Y, Zhu B, Wu D, Wang Q, Yang Y, Ye W, Guo J (2012) Chem Eng J 181–182:387–396
38. Omar HA, Moloukhia H (2008) J Hazard Mater 157:242–246
39. Zaki AA, El-Zakla T, Abed El-Geleel M (2012) J Membr Sci 401–402:1–12